

UNCLASSIFIED

AD NUMBER
AD819319
NEW LIMITATION CHANGE
TO Approved for public release, distribution unlimited
FROM Distribution: Further dissemination only as directed by Air Force Cambridge Research Labs., Hanscom Field, MA, APR 1967, or higher DoD authority.
AUTHORITY
AFCRL ltr, 22 Dec 1971

THIS PAGE IS UNCLASSIFIED

AD819319

AFCL-57-0241
APRIL 1967
PHYSICAL SCIENCES RESEARCH PAPERS, NO. 322



AIR FORCE CAMBRIDGE RESEARCH LABORATORIES

L. G. HANSCOM FIELD, BEDFORD, MASSACHUSETTS

Phase in the Pulsed Radar Time-Stream

C. J. SLETTEN
F. S. HOLT



OFFICE OF AEROSPACE RESEARCH
United States Air Force



This document may be further distributed by any holder only with specific prior approval of CRD, AFCRL, OAR.

Qualified requestors may obtain additional copies from the Defense Documentation Center.

AFCRL-67-0241
APRIL 1967
PHYSICAL SCIENCES RESEARCH PAPERS, NO. 322



MICROWAVE PHYSICS LABORATORY PROJECT 5635

AIR FORCE CAMBRIDGE RESEARCH LABORATORIES

L. G. HANSCOM FIELD, BEDFORD, MASSACHUSETTS

Phase in the Pulsed Radar Time-Stream

C. J. SLETTEN

F. S. HOLT

This document may be further distributed by
any holder only with specific prior approval
of CRD, AFCRL (OAR)

OFFICE OF AEROSPACE RESEARCH
United States Air Force



Abstract

This study is concerned with the identification of certain target characteristics through the analysis of received signals. Signal phase and amplitude as functions of time as well as the frequency spectra characteristics relating to discrete and distributed targets are investigated. The fundamental aspects of information received by a pulsed radar are reexamined with particular emphasis on the possibilities of extracting signature criteria from the signal phase as a function of time when measured relative to an oscillator running at the carrier frequency of the radar. Particular significance is attached to the "stationarity" of the phase for isolated point-targets, compared to the phase variations in the pulse associated with multiple targets entering and leaving the pulse pocket. Coherent phase discontinuities are analyzed in connection with regular distributions of point sources.

Contents

1. INTRODUCTION	1
2. SITUATIONS WHERE ONE-DIMENSIONAL TIME-STREAM ANALYSIS IS USEFUL AND STATEMENT OF ANALYTICAL ASSUMPTIONS	2
3. RESPONSE OF A SINGLE ISOLATED POINT-TARGET, CASE I	5
3.1 Remarks on Case I	6
4. PHASE IN THE TIME-STREAM FOR WIDELY SEPARATED TARGETS, CASE II	7
5. ANALYSIS OF TWO CLOSELY SPACED TARGETS, CASE III	7
5.1 Remarks on Two Targets in a Single Pulse Length	9
6. DISTRIBUTIONS OF RADAR TARGETS CONSIDERED AS ANTENNAS	10
7. THE FORWARD-SCATTER MAXIMA FOR A DISTRIBUTION OF TARGETS	12
8. THE MANY-TARGET PROBLEM WITH REGULARLY DISTRIBUTED IDENTICAL SCATTERERS, CASE IV	13
9. REMARKS ON MORE GENERAL TARGET SITUATIONS	15
10. SIGNAL VARIATIONS CONTROLLABLE BY CHANGES IN CARRIER FREQUENCY OR PULSE LENGTH	16
APPENDIX A. Frequency Spectrum of a Repeating Sequence of Radar Pulses on a Long-Time Basis	A1
APPENDIX B. Frequency Spectrum of a Finite Number of Radar Pulses	B1

Illustrations

1.	Examples of Situations Where a One-Dimensional Model of Back-scattering is Applicable	3
2.	Transmitted Pulsed Carrier and cw Reference Signal	4
3.	Phase vs Time for Widely Separated Point-Targets (Cases I and II)	8
4.	Phase vs Time Chart for Two Point-Targets With Spacing of $c\tau/2$ or Less	8
5.	Forward-Scatter From a Line Distribution of M Point-Scatterers	13
6.	Backscatter From a Line Distribution of Point-Targets	14
7.	Phase vs Time Chart for Many Identical Targets With Uniform Spacing Greater Than $c\tau/2$	15
8.	Cornu-Spiral Representation for One to Five Targets Entering the Pulse	16
9.	Wavelength Dependence of Backscattering From Uniformly Spaced Targets	18
10.	Behavior of Signal Amplitude for a Uniform Line Distribution of Periodic Targets Extending Over a Length Greater Than $c\tau/2$	19
B1.	Plot of Amplitude of Frequency Spectrum for a Single Radar Pulse With $T \gg 1/\omega_0$	B2
B2.	Plot of $H(\omega) = \frac{\sin \left[\frac{N}{2} (\omega - \omega_0) \tau_0 \right]}{\sin \left[\frac{1}{2} (\omega - \omega_0) \tau_0 \right]}$, the Second Factor in Eq. (B4)	B3

Phase in the Pulsed Radar Time-Stream

1. INTRODUCTION

When a radar pulse passes over a point-target such as a resonant dipole about $\lambda/2$ in height or over a distributed surface of resonant or nonresonant scatterers, a different quality of echoes or sequence of echoes is received back at the radar site. It is hoped that, by analyzing the signal events as a function of time for models representing different distributions of scatterers, characteristics helpful for distinguishing the nature of the reflecting objects can be predicated. In particular, the phase, as a function of time following the launch of either a rectangular pulse or a step function of cw wave of carrier frequency ω , is examined with the aim of noting time rate of change of phase which is related to the spectra content of the scattered waves. The process is essentially one of convolving a moving pulse with a distribution of scatterers. Time-domain arguments appear to provide the best insights when searching for signature criteria, making use of phase and amplitude plotted as time functions.

Transient effects are examined in Appendixes A and B. They show that the spectral components are continuous for a single pulse or step and discrete for a constantly repeated pulse. This kind of spectral analysis is rigorous and, because operations are mathematically linear, allows treatment of many target situations

(Received for publication 14 April 1967)

by superposition. Radars usually work in nondispersive media with very wideband amplifiers, so the mathematical assumption that the spectrum due to complex target characteristics can be superimposed on the pulsed spectrum is approximately realizable.

Fourier methods which concentrate on spectrum usually discard the signature information contained in the time stream in both the phase vs time and amplitude vs time functions. For lower frequency radars, the phase vs time function can be measured; it yields important information about the targets. The spectrum analysis methods inextricably combine the amplitude and phase parameters and critically depend on the number of repeated observations, as indicated in the appendixes by the examples worked out on a short-time and long-time basis.

Results of the time-domain analysis also suggest certain processing circuitry for identifying returns for various classes of targets. This simple treatment is easily and rigorously related to the physics of the problems and is experimentally verifiable when transmitters produce pulses with very sharp rise and cut-off times, free of FM, and the receivers are very wideband and receive signals with high signal-to-noise levels.

When either a cw or a pulsed cw electromagnetic wave of frequency ω is reflected from a fixed point-target and then beat with the same cw source back at the launch point of the wave, a constant phase shift is observed. This can be verified by noting that a fixed standing wave exists around the launch region under these conditions. It is also well recognized that when the target or the radar is in uniform motion, a linear phase shift with time or Doppler frequency shift is observed. The relative phase function $\Phi(t)$ will be calculated, as recorded at the transmitter location, for a pulsed radar with pulses (usually) containing many cycles of rf at frequency ω .

A sequence of phase delays that produce mainly asymmetric "lower side bands" might be expected because a propagating pulse excites targets progressively later in time. It is assumed that phase comparison of the return signal against one frequency component, the cw carrier, will yield interpretable information. Such an approach was successful in studying pulse dispersion in waveguides by M. Ito (1936). (See IEEE, PGMTT, May 1955.)

2. SITUATIONS WHERE ONE-DIMENSIONAL TIME-STREAM ANALYSIS IS USEFUL AND STATEMENT OF ANALYTICAL ASSUMPTIONS

Examples of situations in which one-dimensional radar reflections can be well approximated by pulsed echoes are shown in Figure 1.

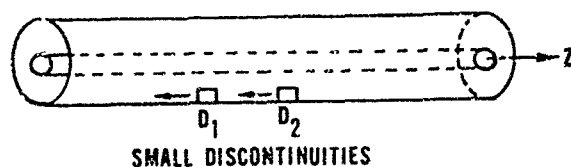


Figure 1a. Transmission Line

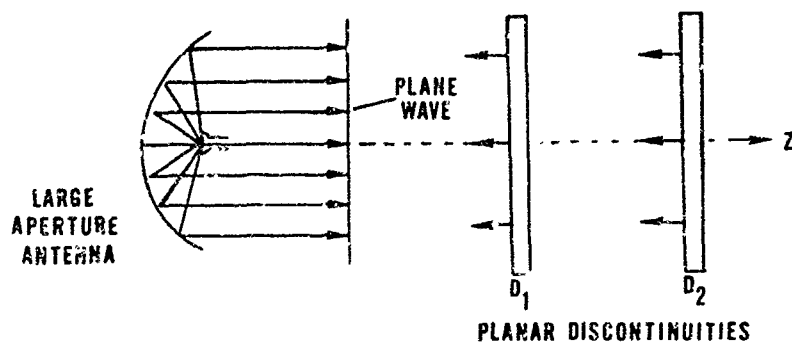


Figure 1b. Near Zone of Large Antenna

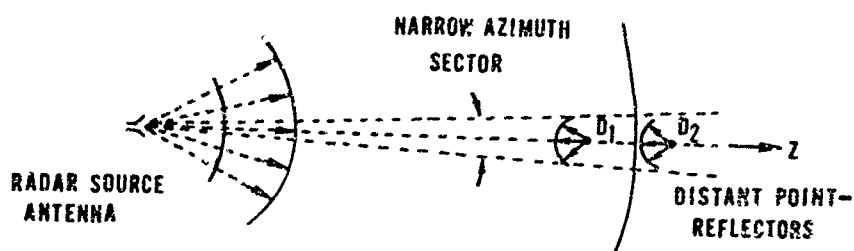


Figure 1c. Far Field Radar Problem

Figure 1. Examples of Situations Where a One-Dimensional Model of Backscattering is Applicable

It will be assumed that the phase velocity is everywhere constant and equal to c , the velocity of light. Then, of course, $\beta = 2\pi/\lambda$, $c = f\lambda$, and $\omega = 2\pi f = 2\pi/T$. The transmitted cw waves will be considered plane at regions of discontinuities and represented as a single frequency plane wave of E field,

$$E(t, z) = \frac{E_0}{z} e^{j(\omega t - \beta z)},$$

such that the phase is constant for an observer moving with the wave at velocity $c = \omega/\beta$.

Introducing a rectangular pulse of time duration τ containing several sine-wave cycles at frequency ω (see Figure 2), and concentrating attention only on the phase and strength of spectral component ω , the transmitted pulse is written

$$E(t, z) = \begin{cases} 0 & , t - \frac{\beta z}{\omega} < \epsilon \\ Ae^{j(\omega t - \beta z)} & , 0 + \epsilon < t - \frac{\beta z}{\omega} < \tau - \epsilon \\ 0 & , \tau - \epsilon < t - \frac{\beta z}{\omega} \end{cases}$$

where t is measured from the leading-edge launch time $t = 0$ at $z = 0$. The time interval ϵ is introduced to indicate that transient effects viewed in the time domain measured at z alter the representation near the times $t = \beta z / \omega$ and $t = (\beta z / \omega) + \tau$, where the function is assumed discontinuous. These time intervals can be made relatively small by increasing either the pulse length or the system bandwidth, or both, and will be omitted in the discussions to follow.

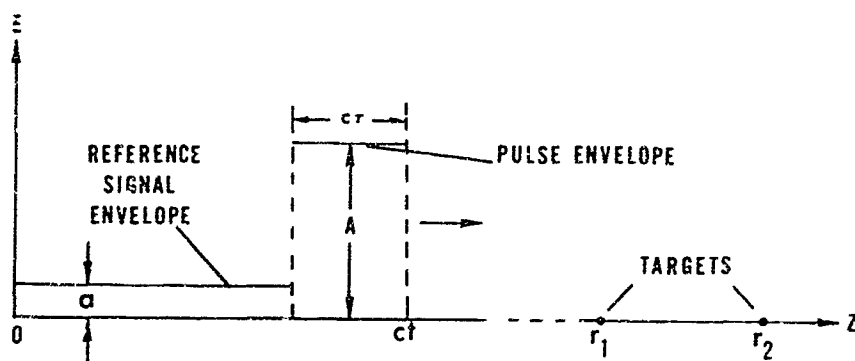


Figure 2. Transmitted Pulsed Carrier and cw Reference Signal

It will be assumed that the distance interval in which all targets are located is very small compared to the range from $z = 0$ (backscatter) or from $z = R$ (forward-scatter); hence, signal variation from target to target due to range attenuation will be neglected. Thus, in each case to be considered the factor A will be assumed constant.

It is also assumed that a reference signal continuing at a level $a \ll A$ will be used to beat with the back-scattered signals, or

$$E_{\text{cw}} = a e^{j(\omega t - \beta z)}, \quad t > \tau$$

reference

3. RESPONSE OF A SINGLE ISOLATED POINT-TARGET, CASE I

Consider a wave pulse launched from $z = 0$ at $t = 0$ and reflected from a target located at $z = r_1$ (see Figure 2). The reflected signal will be

$$E_1(t, z) = \begin{cases} 0 & , \quad t + \frac{\beta z}{\omega} < t_1 \\ A a_1 e^{j(\omega t + \phi_1 + \beta z - 2\beta r_1)} & , \quad t_1 < t + \frac{\beta z}{\omega} < t_1 + \tau \\ 0 & , \quad t_1 + \tau < t + \frac{\beta z}{\omega} \end{cases}$$

where $a_1 e^{j\phi_1}$ is the reflection coefficient of the target and

$$t_1 = \frac{2\beta r_1}{\omega} = \frac{2r_1}{c}$$

Adding the reference signal to the reflected signal yields

$$E_{\text{cw}} + E_1(t, z) = \begin{cases} a e^{j(\omega t - \beta z)} & , \quad \tau + \frac{\beta z}{\omega} < t + \frac{\beta z}{\omega} < t_1 \\ \left[a e^{j(\omega t_1 - \beta z)} + A a_1 e^{j(\phi_1 + \beta z)} \right] e^{j\omega(t-t_1)} & , \quad t_1 < t + \frac{\beta z}{\omega} < t_1 + \tau \\ a e^{j(\omega t - \beta z)} & , \quad t_1 + \tau < t + \frac{\beta z}{\omega} \end{cases}$$

It is now assumed that $a = A a_1$ and noted that the sum of the signals produces a standing wave in the z interval

$$\frac{\omega}{\beta} (t_1 - t) < z < \frac{\omega}{\beta} (t_1 + \tau - t)$$

The nulls of this standing wave are fixed at those values of z that lie in the above interval and satisfy the equations

$$\omega t_1 - \beta z = \phi_1 + \beta z \pm n\pi, \quad n = 1, 3, 5, \dots$$

Thus at any point z , the relative phase—that is, the phase of the reflected signal relative to the phase of the reference signal—is constant during the time interval

$$t_1 - \frac{\beta z}{\omega} < t < t_1 + \tau - \frac{\beta z}{\omega}.$$

In particular, at $z = 0$ the relative phase is constant during the time interval

$$t_1 < t < t_1 + \tau.$$

3.1 Remarks on Case (

When a single point-target is located at $z = r_1$, accurately measuring the stationary phase of the reflected signal relative to the reference signal can give accurate range data on the target position for situations where good clocks or gating circuits are available to establish t_1 to within a period $T = \frac{2\pi}{\omega}$. Although phase information has seldom been employed to find range or arrival time of pulses, it should be noted that for a broadband system this constant phase will be maintained for a large fraction of the pulse time τ and, furthermore, the information is repeated on succeeding pulses.

Conversely, if t_1 can be accurately measured and the phase $(\omega t_1 - n\pi)$ is known, then theoretical means exist for establishing $a_1 e^{j\phi_1}$, where ϕ_1 is the phase shift introduced by the reflection coefficient of the target on the carrier frequency component. This phase shift may be different for metal resonant (dipole-like) objects than for lossy or nonresonant objects.

Scattering from objects, especially high-Q resonant objects, can be frequency dependent or dispersive. One could examine the pulse distortion (amplitude) as a function of time to see how the frequency components in the pulse are phase shifted and attenuated in the scattering with a resonant object. This is difficult as most radiating metal objects have low-Q as scatterers; therefore, it is advantageous to concentrate on the phase of the ω frequency region that contains most of the energy.

For target discrimination, the stationary-phase characteristic of a point-target should be noted. Only a single isolated point-target has this property. When the phase in the time-stream of echoes stays constant for nearly a time τ , an isolated point-target is identified.

4. PHASE IN THE TIME-STREAM FOR WIDELY SEPARATED TARGETS, CASE II

In addition to a target at $z = r_1$, suppose that a second target is located at $z = r_2$ (see Figure 2), where $\frac{r_2 - r_1}{c}$ is greater than a half pulse length, and assume that this second target with reflection coefficient $a_2 e^{j\phi_2}$ reflects a pulse that arrives back at our phase-comparison device at $t = t_2$. It will now be assumed that phase will be measured by means other than locating null positions (the VSWR method) in the vicinity of $z = 0$. The total field at $z = 0$ due to the returns from the point-targets at r_1 and r_2 can be written as

$$E_1(t, 0) + E_2(t, 0) = \begin{cases} 0 & , t < t_1 \\ A \left[a_1 e^{j(\phi_1 - 2\beta r_1)} \right] e^{j\omega t} & , t_1 < t < t_1 + \tau \\ 0 & , t_1 + \tau < t < t_2 \\ A \left[a_2 e^{j(\phi_2 - 2\beta r_2)} \right] e^{j\omega t} & , t_2 < t < t_2 + \tau \\ 0 & , t_2 + \tau < t \end{cases}$$

The phase at $z = 0$ of the total reflected field relative to the reference signal as a function of time is shown graphically in Figure 3.

5. ANALYSIS OF TWO CLOSELY SPACED TARGETS, CASE III

Consider now two point-targets separated in range by less than half a pulse length, that is, $0 < \Delta r = r_2 - r_1 < \frac{c\tau}{2}$, but still separated by a large number of wavelengths λ (so that mutual coupling can be disregarded). Again at $z = 0$,

$$E_1(t, 0) + E_2(t, 0) = \begin{cases} 0 & , t < t_1 \\ A \left[a_1 e^{j(\phi_1 - \omega t_1)} \right] e^{j\omega t} & , t_1 < t < t_2 \\ A \left[a_1 e^{j(\phi_1 - \omega t_1)} + a_2 e^{j(\phi_2 - \omega t_2)} \right] e^{j\omega t} & , t_2 < t < t_1 + \tau \quad (1) \\ A \left[a_2 e^{j(\phi_2 - \omega t_2)} \right] e^{j\omega t} & , t_1 + \tau < t < t_2 + \tau \\ 0 & , t_2 + \tau < t \end{cases}$$

and now the signals overlap in three different time intervals. Three time intervals of stationary phase are distinguished as shown in Figure 4.

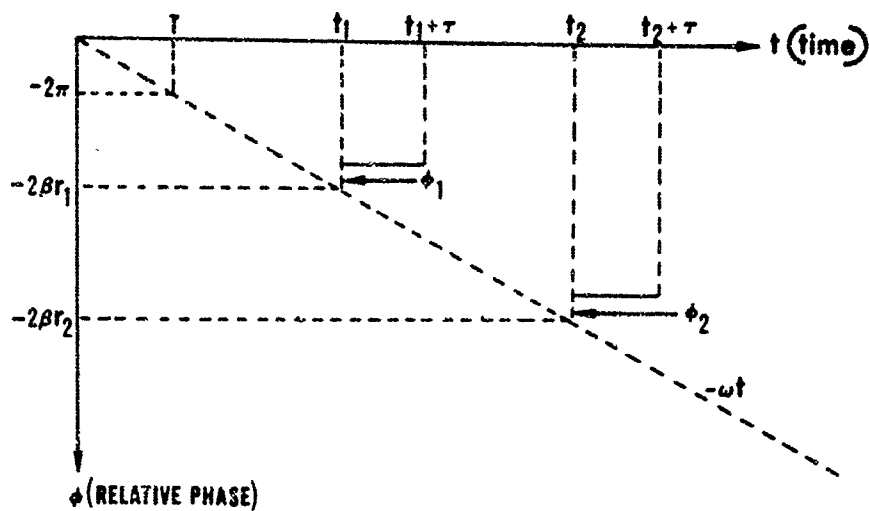


Figure 3. Phase vs Time for Widely Separated Point-Targets (Cases I and II)

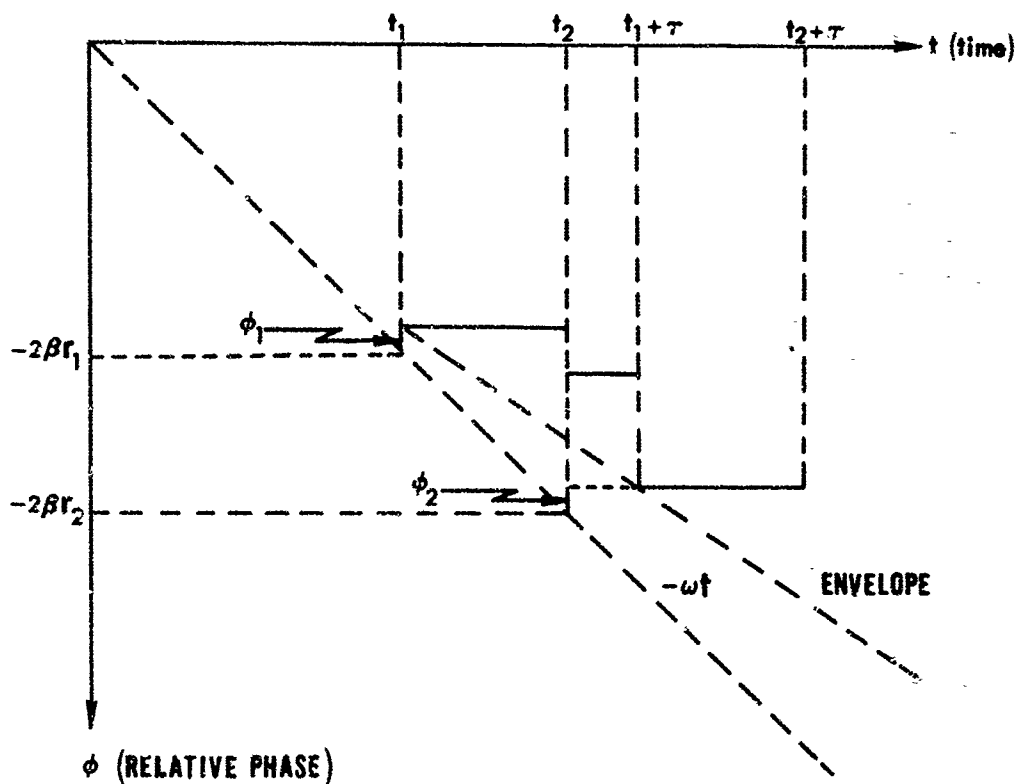


Figure 4. Phase vs Time Chart for Two Point-Targets with Spacing of $c\tau/2$ or Less

5.1 Remarks on Two Targets in a Single Pulse Length

An observer at $z = 0$ doing phase comparison with the phasor $E_{cw} = ae^{j\omega t}$ would note three intervals of stationary phase recognizable by their time of occurrence and duration. From an analysis of these phase intervals, the magnitude and phase of the reflection coefficients and the range to the targets can be determined. An observer doing only phase comparison (with no precise knowledge of time or of the signal strengths Aa_1 and Aa_2) would see precisely two phase jumps (one at t_2 and one at $t_1 + \tau$) and would note that the relative phase does not remain stationary during a whole pulse, τ .

When Aa_1 , Aa_2 , ϕ_1 , and ϕ_2 are measured, the phase jump at t_2 can be calculated from

$$E(t, 0) = A \left[a_1 e^{-j(\omega t_1 - \phi_1)} + a_2 e^{-j(\omega t_2 - \phi_2)} \right] e^{j\omega t}.$$

Consider now the special case of two targets spaced closer than $\lambda/4$ in range. This implies $0 < \omega(t_2 - t_1) < \pi$. Assume also that $Aa_1 = Aa_2 = a$, and $\phi_1 = \phi_2 = 0$. According to Eq. (1) the total returned signal at $z = 0$ is

$$E_1(t, 0) + E_2(t, 0) = \begin{cases} 0 & , t < t_1 \\ ae^{j\omega(t-t_1)} & , t_1 < t < t_2 \\ a \left[e^{j\omega(t-t_1)} + e^{j\omega(t-t_2)} \right] & , t_2 < t < t_1 + \tau \\ ae^{j\omega(t-t_2)} & , t_1 + \tau < t < t_2 + \tau \\ 0 & , t_2 + \tau < t \end{cases} \quad (2)$$

We are interested in calculating the average rate of change of phase of the total returned signal relative to the phase of the cw reference signal over the time interval $t = t_1^+$ to $t = t_2^+$. From Eq. (2) we have at $t = t_2^+$

$$E_1(t_2^+, 0) + E_2(t_2^+, 0) = a \left[e^{j\omega(t_2-t_1)} + 1 \right] = 2ae^{j\frac{\omega}{2}(t_2-t_1)} \cos \left[\frac{\omega}{2}(t_2-t_1) \right]$$

and

$$\arg \left[E_1(t_2^+, 0) + E_2(t_2^+, 0) \right] = \frac{\omega}{2}(t_2-t_1),$$

since $0 < \frac{\omega}{2}(t_2-t_1) < \frac{\pi}{2}$.

Thus, the relative phase at $t = t_2^+$ is

$$\phi(t_2^+) = \arg \left[E_1(t_2^+, 0) + E_2(t_2^+, 0) \right] - \omega t_2 = -\frac{\omega}{2} (t_2 + t_1), \quad 0 < r_2 - r_1 < \frac{\lambda}{4}.$$

Also from Eq. (2) we have at $t = t_1^+$,

$$E_1(t_1^+, 0) + E_2(t_1^+, 0) = a;$$

hence, the relative phase at $t = t_1^+$ is

$$\phi(t_1^+) = \arg \left[E_1(t_1^+, 0) + E_2(t_1^+, 0) \right] - \omega t_1 = -\omega t_1.$$

Note that, since $\phi(t)$ is constant for $t_1 < t < t_2$, it follows that

$$\phi(t_2^-) = \phi(t_1^+) = -\omega t_1.$$

Therefore, the average rate of change of relative phase can be written and evaluated as follows:

$$\frac{\Delta\phi}{\Delta t} = \frac{\phi(t_2^+) - \phi(t_1^+)}{t_2 - t_1} = \frac{\phi(t_2^+) - \phi(t_2^-)}{t_2 - t_1} = \frac{[\text{Jump in } \phi(t) \text{ at } t = t_2]}{t_2 - t_1} = -\frac{\omega}{2}. \quad (3)$$

This average rate of change, $-\omega/2$, can be interpreted as the slope of the "envelope" curve in Figure 4 under the assumed conditions. If the relative phase curve followed the envelope curve over the interval $t_1 < t < t_2$, then a frequency shift of $-\omega/2$ in the returned signal would be expected. In practice the determination of the phase jump would require phase measurement in a time interval of $T/2$, but that is not practical. If the target spacing exceeds $\lambda/4$, then additional phase shifts of $-k\pi$, $k = 0, 1, 2, \dots$ are present, depending on the spacing, and the slope of the envelope curve is no longer $-\omega/2$.

6. DISTRIBUTIONS OF RADAR TARGETS CONSIDERED AS ANTENNAS

Before looking at more general cases of distributed targets characterized by reflection coefficients and geometric arrangements, it will be of value to review the essentials of antenna array theory, which govern parasitic arrays. Consider

the radar return from a sequence of regular reflections (as obtained from regularly spaced trees on the earth) as equivalent to the response of a huge antenna that is progressively excited by a long burst of radio energy. Of primary interest are the back-fire scattering characteristics of this huge surface-wave antenna, with particular attention to both the gain (signal or echo strengths as functions of time) and the phase (especially as a function of time) of the scattered field, treated as an antenna pattern. This is a profitable viewpoint in radar signature analysis.

The field strength of the echoes measured at $z = 0$ for Case III with two targets separated by $\Delta r = r_2 - r_1$ is given (approximately) by

$$E(t, 0) = E_1(t, 0) + E_2(t, 0) = A_0 \left[\frac{a_1}{r_1} e^{-j(\omega t_1 - \phi_1)} + \frac{a_2}{r_2} e^{-j(\omega t_2 - \phi_2)} \right] e^{j\omega t}. \quad (4)$$

In radar studies, the time and phase dependence is usually suppressed, and attention is concentrated on range and amplitude of the radar return. In antenna pattern analysis, time and range attenuation are suppressed and the point-targets are usually assumed to radiate isotropically. If we consider the radiation pattern in the back direction (most used in radar) as a function of target reflection and geometric arrangement, we can write for the field at $z = 0$

$$\begin{aligned} E(t, 0) &= A \left[a_1 e^{-2j\beta r_1} e^{j\phi} + a_2 e^{-2j\beta r_2} e^{j\phi_2} \right] e^{j\omega t} \\ &= A e^{-2j\beta r_1} \left[a_1 e^{j\phi_1} + a_2 e^{-2j\beta \Delta r} e^{j\phi_2} \right] e^{j\omega t}. \end{aligned} \quad (5)$$

Maximum backscattering will occur if there exists some number k , $k = 0, \pm 1, \pm 2, \dots$, such that

$$\phi_1 = \phi_2 - 2\beta \Delta r + 2k\pi = \phi_2 - \frac{4\pi \Delta r}{\lambda} + 2k\pi.$$

This condition will be satisfied and

$$E(t, 0) = |E|_{\max} = |A| (a_1 + a_2)$$

if

$$\Delta r = \frac{\lambda}{2}, \phi_1 = \phi_2, \text{ and } k = 1.$$

The condition for minimum backscattering is that there exist some number k , $k = 0, \pm 1, \pm 2, \dots$, such that

$$\phi_1 = \phi_2 - \frac{4\pi\Delta r}{\lambda} + (2k+1)\pi.$$

Therefore, minimum backscattering will occur if $\phi_1 = \phi_2$ and $\Delta r = \lambda/4$. For identical targets with $\Delta r = \lambda/4$ it follows that

$$E(t, 0) = |E|_{\min} = |A| \cdot |a_1 - a_2| = 0.$$

It is easy to generalize these results for many equally spaced targets. It is well known that in a transmission line identical small reflections spaced $\frac{\lambda_g}{2}$ apart cause very large backscattering or VSWR. Conversely, if λ is selected such that the spacings Δr are $n\lambda/4$ and n is an odd integer, a growth of trees with regular radial spacing should produce a small return on the radial lines about a radar (azimuth bins).

7. THE FORWARD-SCATTER MAXIMA FOR A DISTRIBUTION OF TARGETS

The scattering in other directions, such as broadside and end-fire, was neglected. When thinking about the strength of the return with different modulations (frequency variations with time or partially coherent waves temporally), it is interesting to consider how a beam of electromagnetic energy scatters in all directions. This theme is beyond the scope of this paper, but it can easily be shown that a coherent radar wave always produces strong forward-scatter when exciting similar targets, regardless of their geometric spacing. This is not true for temporally incoherent radar waves.

To illustrate this, forward-scatter (the extinction cross section) at $z = R \gg r_M$ of a line distribution of M point-scatterers is calculated, as shown in Figure 5. The forward-scattered field, measured at $z = R$, will be

$$E(t, R) = Ae^{j\omega t} \sum_{k=1}^M a_k e^{-j\beta r_k} e^{j\phi_k} e^{j\beta(R-r_k)} = Ae^{j(\omega t - \beta R)} \sum_{k=1}^M a_k e^{j\phi_k}.$$

Note that $E(t, R)$ is independent of all the r_k 's. When $\phi_k = \phi_0$ for all k , then the forward-scatter will be maximum and will equal $|A| (a_1 + a_2 + \dots + a_M)$.

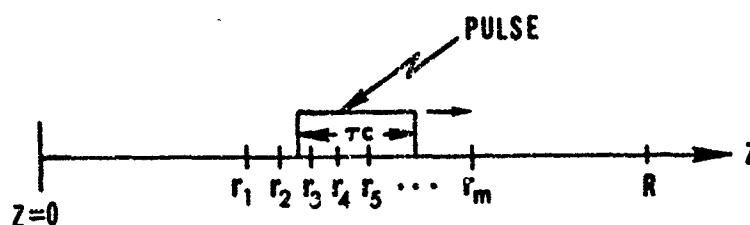


Figure 5. Forward-Scatter From a Line Distribution of M Point-Scatterers

8. THE MANY-TARGET PROBLEM WITH REGULARLY DISTRIBUTED IDENTICAL SCATTERERS, CASE IV

Attention is again turned to radar backscattering from a surface with a distribution of point-scatterers, where it is desired to interpret the nature and configuration of these scatterers by studying phase in the time-stream; also considered are the effects of variation in ω or τ to either maximize or minimize the amplitude of the scattering from target configurations. Variations in propagation velocity c are still neglected, although a reactive surface ($\phi_k \neq 0$) will support a trapped surface wave when its velocity v is less than c as on a yagi antenna. It is assumed that a plane wave travelling at $v = c$ drives or excites the scatterers. This assumption is a good approximation of an airborne radar illuminating the earth from a high altitude.

Consider the backscattering phase vs time function for a periodic scattering surface made up of many scatterers regularly spaced and of equal reflection coefficients, $ae^{j\phi}$ (see Figure 6). The returned signal from N targets measured at $t = t_n$ is

$$E(t_n, 0) = Aae^{j\phi} e^{j\omega t_n} \sum_{k=0}^{N-1} e^{-j\omega t_n - k} = Aae^{j\phi} e^{j\omega(\frac{N-1}{2}) \Delta t} \frac{\sin(\frac{\omega N \Delta t}{2})}{\sin(\frac{\omega \Delta t}{2})},$$

where t_n is the time when the echo from the target at $z = r_n$ first returns to $z = 0$. This returned signal will be compared to the reference phasor $E_{cw} = Aae^{j\omega t}$.

For uniform regular spacing we can write

$$r_i - r_{i-1} = \Delta r_i = \Delta r$$

$$t_i - t_{i-1} = \Delta t.$$

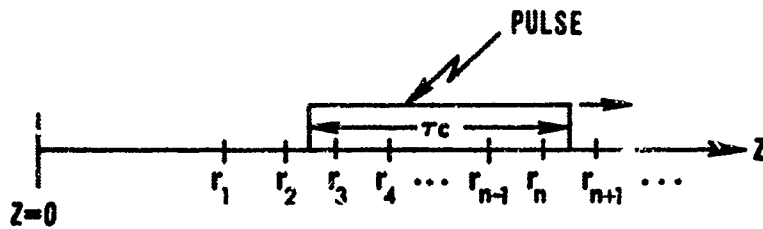


Figure 6. Backscatter From a Line Distribution of Point-Targets

It will be assumed that at all times the transmitted pulse of length τ illuminates precisely two N targets. Then at any instant the signal received at $z = 0$ is the sum of the echoes from precisely N targets. Thus,

$$N\Delta r = \frac{c\tau}{2}, \quad \Delta r = \frac{c\Delta t}{2}, \quad \text{and} \quad N\Delta t = \tau.$$

We wish to calculate the average rate of change of the relative phase of the returned signal over the time interval $t_n < t < t_{n+1}$. Now

$$\begin{aligned} E(t_{n+1}, 0) &= Aae^{j(\phi + \omega t_{n+1})} \sum_{k=0}^{N-1} e^{-j\omega t_{n+1-k}} \\ &= Aae^{j(\phi + \omega t_n)} \sum_{k=0}^{N-1} e^{-j\omega [t_{n+1-k} - (t_{n+1} - t_n)]} \\ &= Aae^{j(\phi + \omega t_n)} \sum_{k=0}^{N-1} e^{-j\omega t_{n-k}} \\ &= E(t_n, 0). \end{aligned}$$

Thus, the relative phase at $t = t_{n+1}$ is

$$\phi(t_{n+1}) = \arg [E(t_{n+1}, 0)] - \omega t_{n+1}$$

and at $t = t_n$ is

$$\phi(t_n) = \arg [E(t_n, 0)] - \omega t_n.$$

The average rate of change of relative phase over the interval $t_n < t < t_{n+1}$ is, therefore,

$$\frac{\Delta\phi}{\Delta t} = -\frac{\omega(t_{n+1} - t_n)}{\Delta t} = -\omega.$$

Any periodic structure will have a large zero frequency component of scattering independent of pulse length as $\Delta r \rightarrow 0$ and $\Delta t \rightarrow 0$. This situation is illustrated with the phase-time diagram (see Figure 7). Thus, under the conditions assumed, a very large or infinite periodic structure acts like point-targets spaced further apart than τ (Case II) and has a phase vs time envelope curve that corresponds to a nonradiating frequency. This loading up of phase by amount $\left[(N-1)/2\right] \omega \Delta t + \phi$ might be detected by long-line effects as ω is varied.

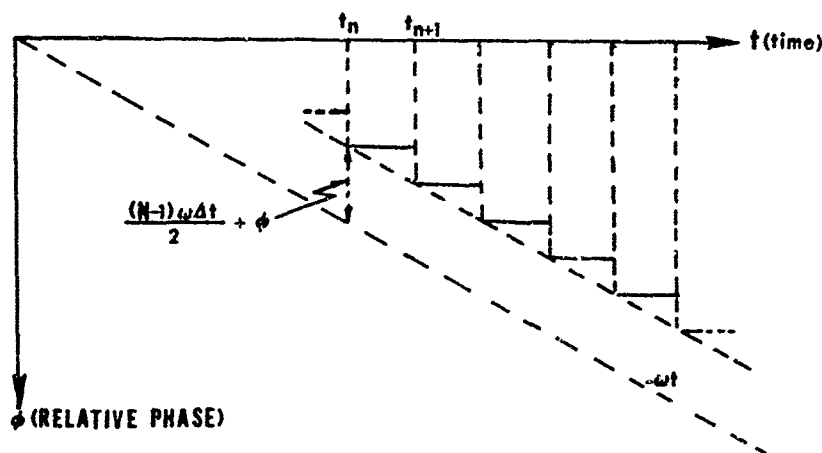


Figure 7. Phase vs Time Chart for Many Identical Targets With Uniform Spacing Greater Than $c\tau/2$

9. REMARKS ON MORE GENERAL TARGET SITUATIONS

A strong target in nearly homogeneous clutter should have a much more stationary phase characteristic than the clutter alone. To analyze general cases it is helpful to use Cornu-spiral representations. Eq. (4) can be expressed more generally as

$$E(t_n, 0) = \sum_{k=1}^n E_k(t_n, 0) = Ae^{j\omega t_n} \sum_{k=1}^n a_k e^{-j(\omega t_k + \phi_k)}.$$

The phase of $E(t_n, 0)$ relative to $E_{cw}(t_n, 0)$ is given by the phase of the vector $E(t_n, 0)e^{-j\omega t_n}$ and is shown in Figure 8 for the cases $n = 1, 2, 3, 4$, and 5.

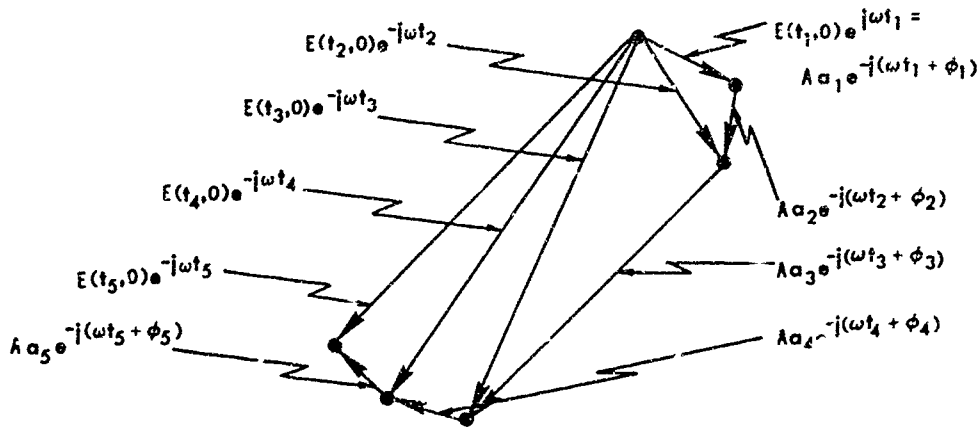


Figure 8. Cornu-Spiral Representation for One to Five Targets Entering the Pulse

If $a_3 \gg a_k$, $k \neq 3$ (as might occur for a resonant metal target in clutter), then the reflected signal $E_3(t_n, 0)$ that arrives at $z = 0$ at $t = t_3$ causes an appreciable shift in the relative phase (and amplitude) of $E(t_n, 0)$. (See Figure 8.) As long as the return from the scatterer at $z = r_3$ is being received at $z = 0$, the addition or subtraction of other target returns (being much smaller than Aa_3) will not rapidly change the phase of $E(t_n, 0)$.

10. SIGNAL VARIATIONS CONTROLLABLE BY CHANGES IN CARRIER FREQUENCY OR PULSE LENGTH

In this section the influence of pulse length and frequency variations on the amplitude signature function for various regular periodic scattering structures are discussed. A pulse that at each instant excites precisely $2N$ uniformly spaced identical targets with reflection coefficients $ae^{j\phi}$ has an echo at $t_n = 2\beta r_n / \omega$, according to Eq. (6) given by

$$E(t_n, 0) = Aae^{j(\phi + \omega t_n)} \sum_{k=0}^{N-1} e^{-j\omega t_{n-k}} = Aae^{j\phi} e^{j\omega(\frac{N-1}{2})\Delta t} \left[\frac{\sin(\frac{\omega N \Delta t}{2})}{\sin(\frac{\omega \Delta t}{2})} \right],$$

where $\Delta t = t_n - t_{n-1}$. If $\Delta r = r_n - r_{n-1}$ is the element spacing and τ is the pulse length, then

$$\frac{4\pi\Delta r}{\lambda} = \omega\Delta t ,$$

$$\Delta t = \frac{2\Delta r}{c} ,$$

and

$$\tau = N\Delta t .$$

Changes in Δr , ω , and τ affect $E(t, 0)$. The maximum return

$$E_{\max}(t, 0) = |A| a N$$

occurs when

$$\frac{\omega\Delta t}{2} = m\pi , \quad m = 0, 1, 2, \dots$$

A practical case occurs when $m = 1$, that is,

$$\Delta r = \frac{\omega\lambda\Delta t}{4\pi} = \frac{\lambda}{2} .$$

To reduce clutter or $E(t, 0)$ set

$$\sin\left(\frac{\omega N\Delta t}{2}\right) = 0$$

and

$$\sin\left(\frac{\omega\Delta t}{2}\right) \neq 0 .$$

This leads to the condition

$$\frac{\omega\Delta t}{2} = \frac{p\pi}{N} ,$$

where p is an integer, not a multiple of N . For a given target distribution, $\Delta t = \frac{2\Delta r}{c}$ is fixed but τ and ω are variable.

When N is large, which can be realized by increasing the pulse length τ , there will be many minima between the first minimum when spacing goes to zero, that is, $\Delta r \rightarrow 0$, $\Delta t \rightarrow 0$, and the second maximum $\Delta r \rightarrow \lambda/2$ (see Figure 9). When N is large many ripples will occur, but the envelope of the scatter amplitude will drop down to $1/N$ or zero at $\lambda/4$ spacing, depending on whether N is odd or even. Thus, a rather broadband region of low scattering cross section would be predicted for $\Delta r \approx \lambda/4$, and a very strong maximum when spacing or spacing times $\cos \gamma$, where γ is elevation angle, is equal to $\lambda/2$:

$$\Delta r \cos \gamma \approx \frac{\lambda}{2} .$$

These conditions would likely be encountered by radar reflection from water waves or from wooded areas. Single adjustment of frequency may greatly reduce clutter scatter.

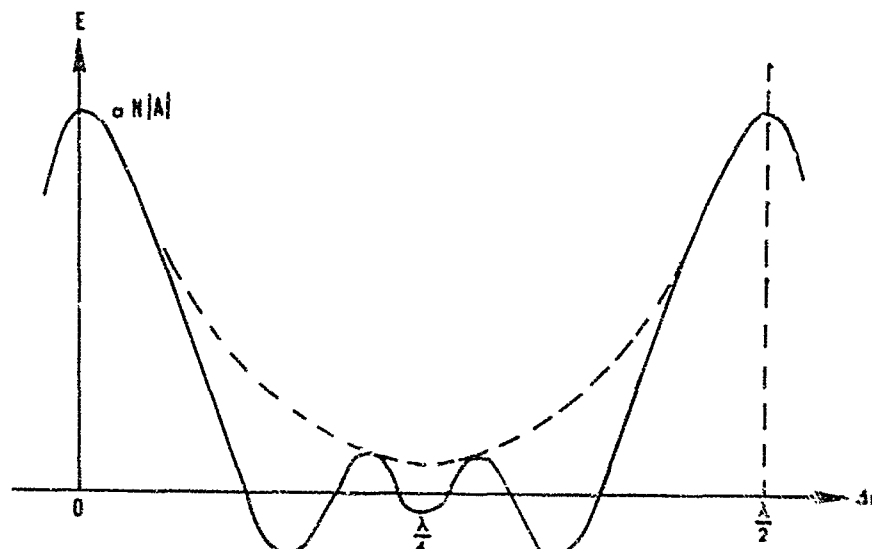


Figure 9. Wavelength Dependence of Backscattering From Uniformly Spaced Targets

The amplitude of the echo stream for a long pulse entering and leaving a periodic structure of scatterers will be

$$|E(t, 0)| = \left| \frac{Aa \sin\left(\frac{\omega M \Delta t}{2}\right)}{\sin\left(\frac{\omega \Delta t}{2}\right)} \right| ,$$

where M is the total number of targets contributing to the echo at the time the signal returns to $z = 0$. This function will have a maximum equal to $|A| aM$ when $\frac{\omega \Delta t}{2} = \pi$ or $\frac{\lambda}{2} = \Delta r$.

If the pulse length $\tau = N\Delta t \geq N'\Delta t$, where N' is the total number of targets, then M will vary progressively from 0 to N' , remain constant at N' for a time interval $(N - N')\Delta t$, and then decrease to 0. If the periodic row of scatterers is longer than $\frac{c\tau}{2}$, that is, $\tau = N\Delta t < N'\Delta t$, then M will vary in a manner similar to the above case, reaching a maximum of N . With $\Delta r = \frac{\lambda}{2}$ the echo amplitude as a function of time will be as shown in Figure 10.

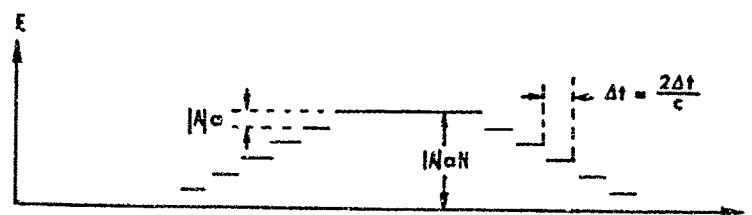


Figure 10. Behavior of Signal Amplitude for a Uniform Line Distribution of Periodic Targets Extending Over a Length Greater Than $c\tau/2$

Appendix A

Frequency Spectrum of a Repeating Sequence of Radar Pulses on a Long-Time Basis

If $f(t)$ is a periodic wave of fundamental frequency $\omega_1 = 2\pi/T_1$ defined over the interval $-\infty < t < \infty$, then it can be expressed as

$$f(t) = \sum_{n=-\infty}^{\infty} A_n e^{jn\omega_1 t} \quad (A1)$$

where

$$A_n = \frac{1}{T_1} \int_0^{T_1} f(t) e^{-jn\omega_1 t} dt . \quad (A2)$$

The frequency spectrum of $f(t)$ will then be discrete and can be expressed in terms of δ -functions as follows:

$$F(\omega) = \int_{-\infty}^{\infty} f(t) e^{-j\omega t} dt = 2\pi \sum_{n=-\infty}^{\infty} A_n \delta(\omega - n\omega_1) . \quad (A3)$$

If now the wave $f(t)$ is truncated for $|t| > T$, then the frequency spectrum becomes

A2

$$F(\omega) = \sum_{n=-\infty}^{\infty} 2A_n T \frac{\sin(\omega - n\omega_1) T}{(\omega - n\omega_1) T} \quad (A4)$$

and is no longer discrete but continuous. In effect each line of the discrete spectrum has been modified in amplitude and spread into a $(\sin \omega T)/\omega T$ shape centered at the spectrum line. The extent of the spreading, that is, the half-power beamwidth of the $(\sin \omega T)/\omega T$ pattern as a function of ω , is inversely proportional to T and, hence, for large T the spectrum can be considered discrete.

In the analysis that follows we will assume that $f(t)$ is either a periodic high-frequency pulse truncated for very large T or a superposition of such pulses displaced in time and phase. Under these conditions the frequency spectrum can be considered discrete and can be closely approximated by Eq. (A3). If in the fundamental period $0 \leq t < T_1$, $f(t)$ is given as follows:

$$f(t) = \begin{cases} u_0 e^{j(\omega_0 t + \phi_0)} & , 0 \leq t < pT_1 \\ 0 & , pT_1 < t < T_1 \end{cases}$$

and

$$2\pi\omega_0 = T_0 \ll T_1 \ll T$$

then Eq. (A3) becomes

$$F(\omega) = 2\pi \sum_{n=-\infty}^{\infty} C_n \delta(\omega - n\omega_1)$$

where

$$C_n = \frac{2 u_0 \sin\{(1/2)pT_1(\omega_0 - n\omega_1)\}}{T_1(\omega_0 - n\omega_1)} e^{j\{(1/2)pT_1(\omega_0 - n\omega_1) + \phi_0\}}$$

If $g(t)$ is $f(t)$ shifted in time by τ , then

$$g(t) = f(t - \tau) = \begin{cases} 0 & , 0 \leq t < \tau \\ u_0 e^{j(\omega_0 t + \phi_0)} e^{-j\omega_0 \tau} & , \tau \leq t < pT_1 + \tau \\ 0 & , pT_1 + \tau < t < T_1 \end{cases}$$

and $G(\omega)$, the frequency spectrum of $g(t)$, is given by

$$G(\omega) = 2\pi \sum_{n=-\infty}^{\infty} D_n \delta(\omega - n\omega_1)$$

where

$$D_n = e^{-j\omega\tau} C_n = \frac{2u_0 \sin\{(1/2)p T_1 (\omega_0 - n\omega_1)\}}{T_1 (\omega_0 - n\omega_1)} e^{j\{(1/2)p T_1 (\omega_0 - n\omega_1) + \phi_0 - \omega\tau\}}$$

Note that the locations of the spectral lines $\omega_n = n\omega_1$ depend only on the pulse repetition frequency ω_1 and not on the high frequency ω_0 , the high-frequency phase ϕ_0 , the time location of the initial value of the pulse τ , or the pulse length pT_1 . Hence, the superposition of additional pulses of different high frequency, different high-frequency phases, different time locations of initial values, and different pulse lengths will not change the spectral line locations.

It is apparent that spectral analysis on a long-time basis will not produce significant information of the type we seek. We next consider spectral analysis on a short-time basis.

Appendix B

Frequency Spectrum of a Finite Number of Radar Pulses

Let $f(t)$ be a single radar frequency pulse as follows:

$$f(t) = \begin{cases} \cos(\omega_0 t + \phi_0) & , |t - \tau| < T \\ 0 & , |t - \tau| > T \end{cases} \quad (B1)$$

The radar frequency is ω_0 , the pulse is centered at time $T = \tau$, and the pulse length is $2T$. The frequency spectrum of this pulse is

$$F(\omega) = \left\{ \frac{\sin[(\omega - \omega_0)T]}{(\omega - \omega_0)} e^{j(\omega_0 \tau + \phi_0)} + \frac{\sin[(\omega + \omega_0)T]}{(\omega + \omega_0)} e^{-j(\omega_0 \tau + \phi_0)} \right\} e^{-j\omega \tau} \quad (B2)$$

Provided $T \gg 1/\omega_0$, that is, provided there are many cycles of the radar frequency in one pulse length, the amplitude of $F(\omega)$ is as shown in Figure B1. Note that the results for $|F(\omega)|$ as shown in Figure B1 are essentially independent of τ and ϕ_0 .

B2

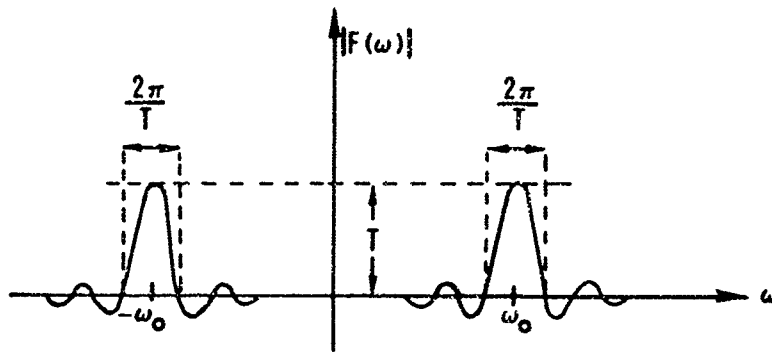


Figure B1. Plot of Amplitude of Frequency Spectrum for a Single Radar Pulse With $T \gg 1/\omega_0$

Now consider the case of N equally spaced radar pulses with $\tau_n = n\tau_0$, $\phi_n = \phi_0$, $n = 0, 1, 2, \dots, N-1$. The spectrum of the superposition of these pulses is

$$\sum_{n=0}^{N-1} F_n = \frac{\sin \left[(\omega - \omega_0) T \right]}{(\omega - \omega_0)} e^{j\phi_0} \sum_{n=0}^{N-1} e^{-jn\tau_0 (\omega - \omega_0)} + \frac{\sin \left[(\omega + \omega_0) T \right]}{(\omega + \omega_0)} e^{-j\phi_0} \sum_{n=0}^{N-1} e^{-jn\tau_0 (\omega + \omega_0)}$$

or

$$\sum_{n=0}^{N-1} F_n = \frac{\sin \left[(\omega - \omega_0) T \right]}{(\omega - \omega_0)} \frac{\sin \left[\frac{N}{2} (\omega - \omega_0) \tau_0 \right]}{\sin \left[\left(\frac{\omega - \omega_0}{2} \right) \tau_0 \right]} e^{-j \left[\frac{N-1}{2} (\omega - \omega_0) \tau_0 - \phi_0 \right]} + \frac{\sin \left[(\omega + \omega_0) T \right]}{(\omega + \omega_0)} \frac{\sin \left[\frac{N}{2} (\omega + \omega_0) \tau_0 \right]}{\sin \left[\left(\frac{\omega + \omega_0}{2} \right) \tau_0 \right]} e^{-j \left[\frac{N-1}{2} (\omega + \omega_0) \tau_0 + \phi_0 \right]} \quad (B3)$$

Again, if $T \gg 1/\omega_0$, then for $\omega > 0$

$$\left| \sum_{n=0}^{N-1} F_n \right| \approx \left| \frac{\sin \left[(\omega - \omega_0) T \right]}{(\omega - \omega_0)} \frac{\sin \left[\frac{N}{2} (\omega - \omega_0) \tau_0 \right]}{\sin \left[\left(\frac{\omega - \omega_0}{2} \right) \tau_0 \right]} \right| \quad (B4)$$

We are most interested in the case where all pulses overlap the initial pulse, that is, $N\tau_0 < 2T$. The first factor in Eq. (B4) is the same as the single pulse result. The form of the second factor for the case $N = 10$ is shown in Figure B2. Since for $\omega > 0$ both factors are symmetrical with respect to $\omega = \omega_0$ and have their peak values at this point, their product will be symmetrical with respect to $\omega = \omega_0$ and will have its peak value NT at this point. The condition $N\tau_0 < 2T$ implies $\frac{4\pi}{N\tau_0} > \frac{2\pi}{T}$ and hence, from Figures B1 and B2, we conclude that the first zeros of Eq. (B4) will occur at the first zeros of the first factor, that is, at $\omega = \omega_0 \pm \pi/T$. The function of Eq. (B4) will lie between the curves

$$G_{\pm}(\omega) = \pm \frac{NT \sin[(\omega - \omega_0) T]}{(\omega - \omega_0) T},$$

becoming tangent to these bounds at $\omega = \omega_0 \pm \frac{2m\pi}{\tau_0}$, $m = 0, \pm 1, \pm 2, \dots$

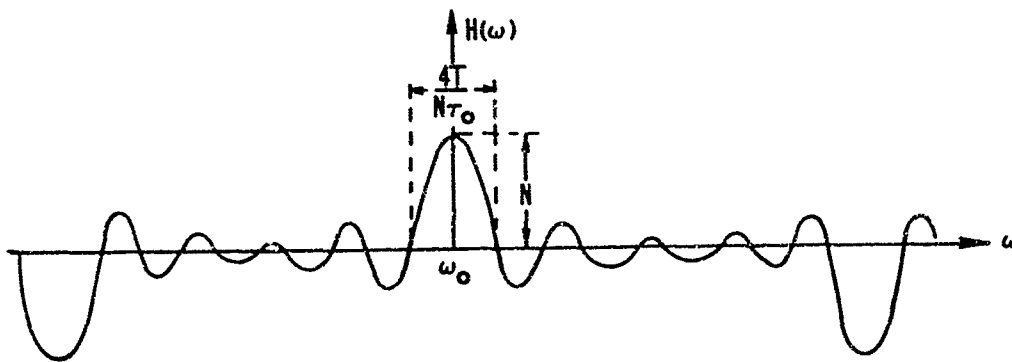


Figure B2. Plot of $H(\omega) = \frac{\sin \left[\frac{N}{2} (\omega - \omega_0) \tau_0 \right]}{\sin \left[\frac{1}{2} (\omega - \omega_0) \tau_0 \right]}$, the Second Factor in Eq. (B4)

Unclassified
Security Classification

DOCUMENT CONTROL DATA - R&D		
(Security classification of title, body of abstract and indexing annotation must be entered when the overall report is classified)		
1. ORIGINATING ACTIVITY (Corporate author) Air Force Cambridge Research Laboratories (CRD) L. G. Hanscom Field Bedford, Massachusetts 01730		2a. REPORT SECURITY CLASSIFICATION Unclassified
		2b. GROUP
3. REPORT TITLE PHASE IN THE PULSED RADAR TIME-STREAM		
4. DESCRIPTIVE NOTES (Type of report and inclusive dates) Scientific Report, Interim.		
5. AUTHOR(S) (First name, middle initial, last name) C. J. Sletten F. S. Holt		
6. REPORT DATE April 1967	7a. TOTAL NO. OF PAGES 31	7b. NO. OF REFS 0
8a. CONTRACT OR GRANT NO.	9a. ORIGINATOR'S REPORT NUMBER(S) AFCRL-67-0241	
b. PROJECT, TASK, WORK UNIT NOS. 5635-05-01		
c. DOD ELEMENT 61445014	9b. OTHER REPORT NO(S) (Any other numbers that may be assigned this report)	
d. DOD SUBELEMENT 681305	PSRP No. 322	
10. DISTRIBUTION STATEMENT This document may be further distributed by any holder only with specific prior approval of AFCRL, OAR (CRD).		
11. SUPPLEMENTARY NOTES		12. SPONSORING MILITARY ACTIVITY Air Force Cambridge Research Laboratories (CRD) L. G. Hanscom Field Bedford, Massachusetts 01730
13. ABSTRACT <p>This study is concerned with the identification of certain target characteristics through the analysis of received signals. Signal phase and amplitude as functions of time as well as the frequency spectra characteristics relating to discrete and distributed targets are investigated. The fundamental aspects of information received by a pulsed radar are reexamined with particular emphasis on the possibilities of extracting signature criteria from the signal phase as a function of the radar. Particular significance is attached to the "stationarity" of the phase for isolated point-targets, compared to the phase variations in the pulse associated with multiple targets entering and leaving the pulse pocket. Coherent phase discontinuities are analyzed in connection with regular distributions of point sources.</p>		

DD FORM 1473
1 NOV 65

Unclassified
Security Classification

Unclassified
Security Classification

14.	KEY WORDS	LINK A		LINK B		LINK C	
		ROLE	WT	ROLE	WT	ROLE	WT
	Radar Antennas Phase Signature Analysis Scattering						

Unclassified
Security Classification